da Silva Gabriel (Orcid ID: 0000-0003-4284-4474)

Self Catalyzed Keto-Enol Tautomerization of Malonic Acid

*Catherine C R Sutton, Chia-Yang Lim, Gabriel da Silva**

Department of Chemical Engineering, The University of Melbourne, Victoria 3010 Australia. *gdasilva@unimelb.edu.au

ABSTRACT

We demonstrate through quantum chemical calculations that the keto-enol tautomerization of malonic acid can be catalysed by the two tautomers of malonic acid itself. This self-catalyzed process proceeds with a relatively low barrier (Gibbs energy *ca*. 13 kcal/mol in gas phase, 20 kcal/mol in aqueous phase), and involves the concerted transfer of two protons between the substrate and the carboxylic acid functionality of the malonic acid catalyst. This mechanism is expected to compete with the proton relay mechanism currently favoured to explain the tautomerization of malonic acid in aqueous media. Malonic acid is an important constituent of secondary organic aerosol (SOA) where the present chemistry may play a role in determining chemical composition.

Keywords: Density functional theory; reaction mechanisms; catalysis

TOC Image

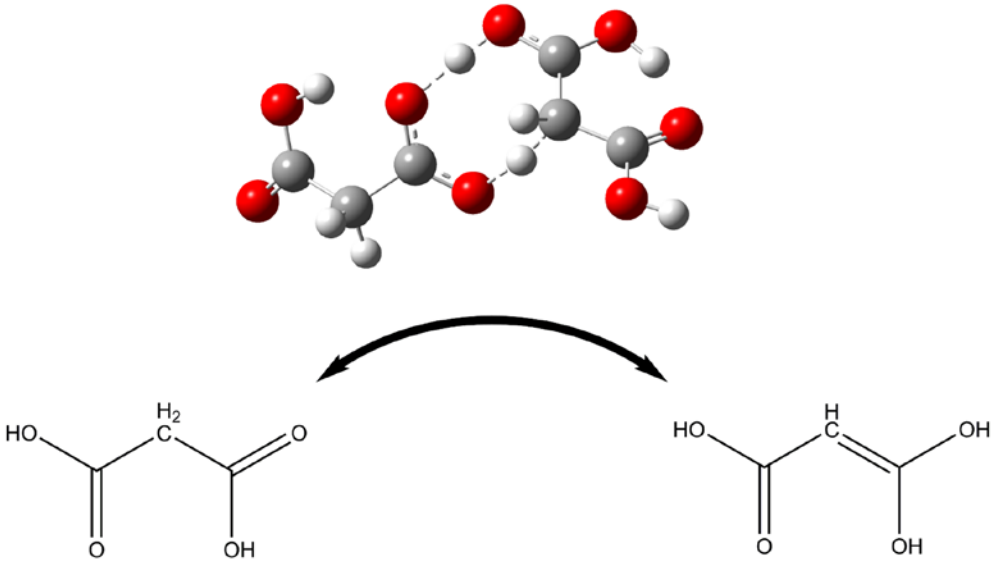

Introduction

Malonic acid, $CH_2(CO_2H)_2$ (Figure 1a), a simple dicarboxylic acid, has been widely studied since the early 20th century primarily due to its usefulness in organic synthesis. Interest in malonic acid has grown in recent years as it has been detected throughout the atmosphere in a variety of locales [1-4],[1-4] in both the gas phase and in aqueous aerosols. Accordingly, a considerable amount of work has been devoted to understanding how malonic acid influences aerosol properties.[5-8] It has long been known that malonic acid can be halogenated, which is interpreted as evidence for the presence of the enol tautomer, $CO_2HCHC(OH)_2$ (Figure 1b).[9] The extent to which this process takes place in the atmosphere, both in the gas phase and in aqueous aerosols, and the effect that this has on aerosol composition, has to date been paid relatively little attention.[10,11]

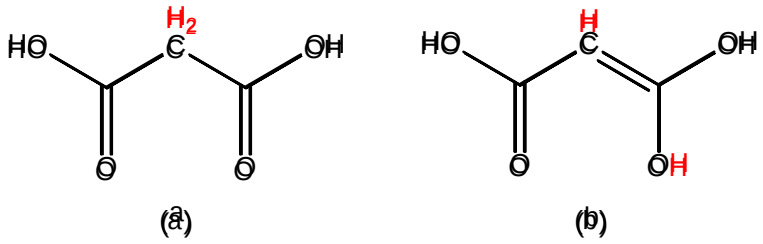

Figure 1: Dicarboxylic acid (a) and enol (b) forms of malonic acid.

Several mechanisms for the keto-enol tautomerization of malonic acid have been proposed, including (i) an intramolecular (direct) proton shift,[9,12] and (ii) a water-mediated proton relay.[13] Initial studies suggested that an intramolecular proton shift was responsible for the tautomerization reaction.[9,12] A number of later studies,[10,13,14] however, showed that the water-mediated proton relay achieves a significant reduction in the barrier height (activation energy of ~16 kcal/mol),[13] and may thus be the primary tautomerization mechanism for malonic acid in the presence of condensed water.

A further mechanism for keto-enol tautomerizations is available,[15] involving concerted movement of two protons between the substrate and an acid catalyst molecule, such as formic acid. Further studies have shown that acid catalyzed double hydrogen atom transfer reactions occur in a wide variety of situations,[16] including other tautomerizations,[17-23] decomposition[24-31] and bimolecular reactions,[32,33] and in keto-enol tautomerizations of dimer complexes.[34,35] Furthermore, this mechanism may also play a role in the isomerization of free radicals,[36] in the hydration of SO_3,[37-40] and in the hydrolysis of carbonyl compounds[41-43] in the atmosphere, as well as in the unimolecular rearrangement of oxygenated volatile organic compounds (VOCs).[44,45]

Malonic acid represents a prototypical compound with a carboxylic acid group that can undergo keto-enol tautomerization, and therefore may undergo self-catalyzed keto-enol tautomerization.[15] As well as being of fundamental interest as an extension of the acid-catalyzed double hydrogen shift mechanism, this process may help to explain the observed tautomerization of malonic acid in solution and in aerosol particles. In this study we have therefore used computational chemistry techniques to investigate this reaction. Quantum chemical calculations were performed using composite wavefunction theory and density functional theory methods, both in the gas phase and in aqueous media (using continuum solvent models).

Computational Methods

All calculations were performed in Gaussian 09.[46] Reported structures were initially optimized at the M06-2X/6-31G(2df,p)[47] density functional theory (DFT) level. Calculations were performed for structures optimized both *in vacuo* and with aqueous media (using IEFPCM,[48] the default polarisable continuum model implemented in Gaussian 09, as well as using SMD).[49] Frequency calculations confirmed all reported minima have no imaginary frequencies and all transition states have a single imaginary mode corresponding to movement between the stated reactants and products. Further to this, intrinsic reaction coordinate scans were used to confirm transition state connectivity to reactants and products. Lowest energy conformers for the dicarboxylic acid and enol forms of malonic acid, as well as the DHS transition states, were identified through a series of optimizations initiated in different starting configurations, as well as through systematic internal rotor scans (for minima). For selected structures, the calculations were also performed at the M05-2X/cc-pVTZ DFT level,[50,51] and higher-level energy calculations were conducted using the composite wavefunction theory (WFT) method G3SX,[52] on the basis of B3LYP/6-31G(2df,p) DFT optimized structures and vibrational frequencies. The reported DFT and composite WFT energies are expected to have mean uncertainties in the range of 2 and 1 kcal/mol, respectively. Energies are reported as electronic energies with zero point energy corrections (*E*+ZPE) and as 298 K enthalpies (*H*) and Gibbs energies (*G*).

Results and Discussion

Conformations of malonic acid and comparison of model chemistries

The seven lowest energy conformers for each of the dicarboxylic acid and enol conformations of malonic acid have been identified and are presented in Table 1. Dicarboxylic acid forms of malonic acid are denoted **K*n*** (the K refers to “keto”) and enol forms of malonic acid are denoted **E*n***. The

most stable enol conformation (**E1**) is around 4 kcal/mol higher in energy than that of malonic acid itself (**K1**). The lowest-energy structures both have one proton from either the carboxylate or enol functionality donating a hydrogen bond into another carboxylate group, with the remaining OH groups undergoing hydrogen bonding with β oxygen atoms.

Table 1: Illustrations of malonic acid conformations, K1 to K6 and E1 to E7 with 298 K relative enthalpies and Gibbs energies. Structures optimized in the gas phase at the M06-2X/6-31G(2df,p) level of theory. Species with a * are involved in the tautomerization pathways described later in this article. E1 is 4.1 kcal/mol higher in enthalpy and 5.2 kcal/mol higher in Gibbs energy than K1.

Dicarboxylic acid conformations				Enol conformations			
	Relative Enthalpy (kcal/mol)	Relative Gibbs Energy (kcal/mol)			Relative Enthalpy (kcal/mol)	Relative Gibbs Energy (kcal/mol)	
K1*	0.0	0.0	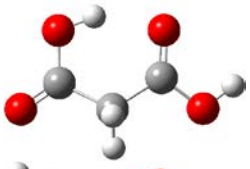	**E1***	0.0	0.0	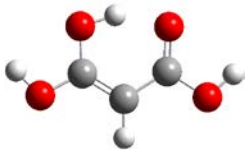
K2	1.1	0.6	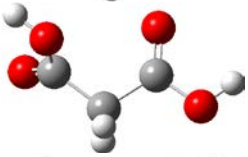	**E2***	2.2	2.1	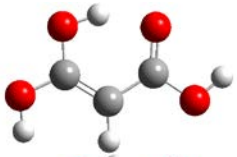
K3	1.2	0.3	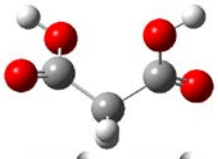	E3	3.7	3.7	
K4*	3.7	3.6	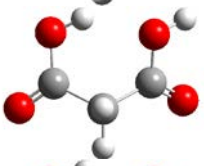	**E4***	7.3	6.7	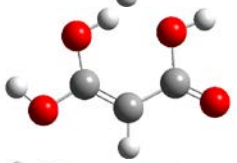
K5	4.8	4.5	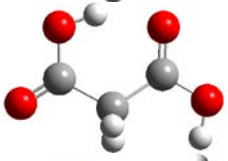	E5	15.0	13.9	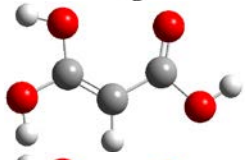
K6	6.5	6.0	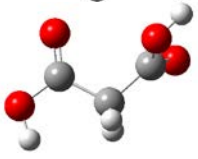	E6	15.5	14.5	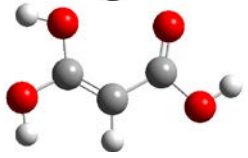

	E7	19.4	18.2	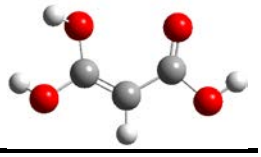

The malonic acid conformations are used to compare the model chemistries and energy calculations. Looking within individual model chemistries, the electronic energies, zero point electronic energies, thermal electronic energies and enthalpies are all very similar.

Comparison of the aqueous models with the gas phase calculation is shown in Figure 2 and Figure 3. For the enol, the order of the relative energies is generally the same as in the gas phase but this is not the case for the dicarboxylic acid conformers K5 to K6, which are significantly lower in energy when modelled in the presence of water.

When comparing across the levels of theory used (i.e. gas to gas, IEF-PCM to IEFPCM and SMD to SMD; see SI 001 to SI 020), it is seen that M05-2X and M06-2X are very similar, although there is some variation in the Gibbs energies for dicarboxylic acid conformations.

Overall, all levels of theory follow similar trends (some variations in exact order of energies). For the remainder of this article, M06-2X energies will be reported for gas and aqueous calculations, with G3SX energies also reported in the gas phase.

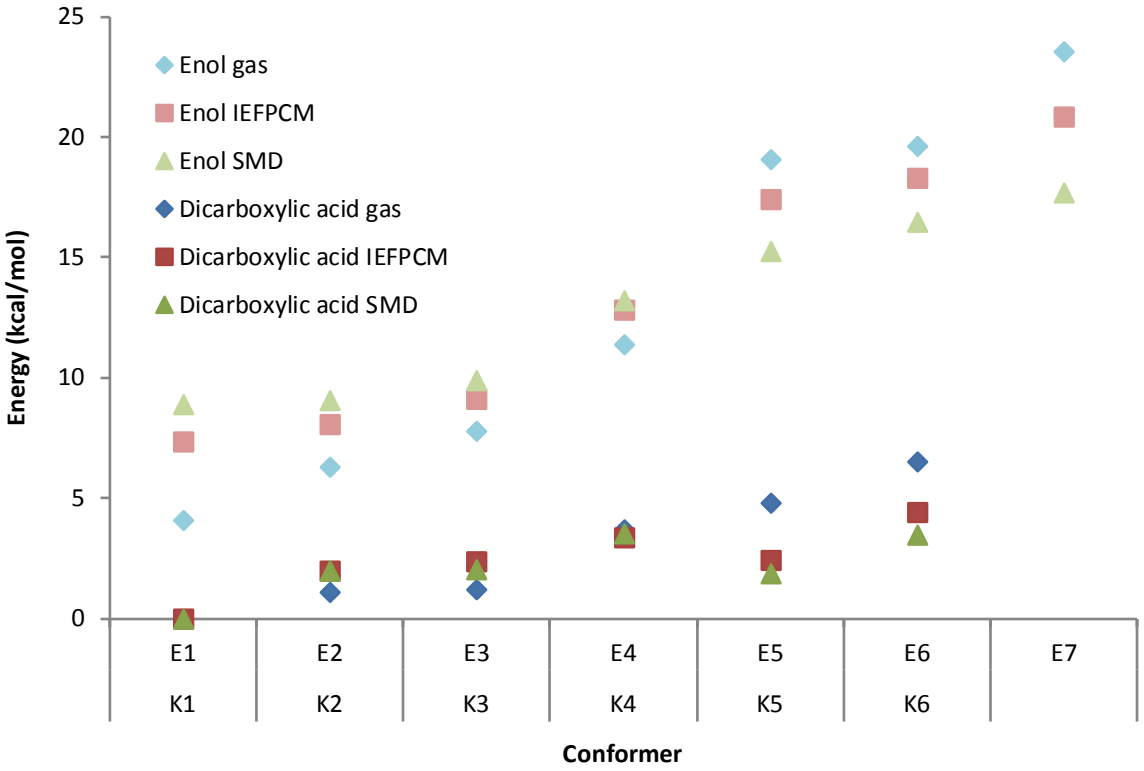

Figure 2: Enthalpy of dicarboxylic acid and enol conformations of malonic acid, calculated at M06-2X. See Table 1 for illustrations of the conformers.

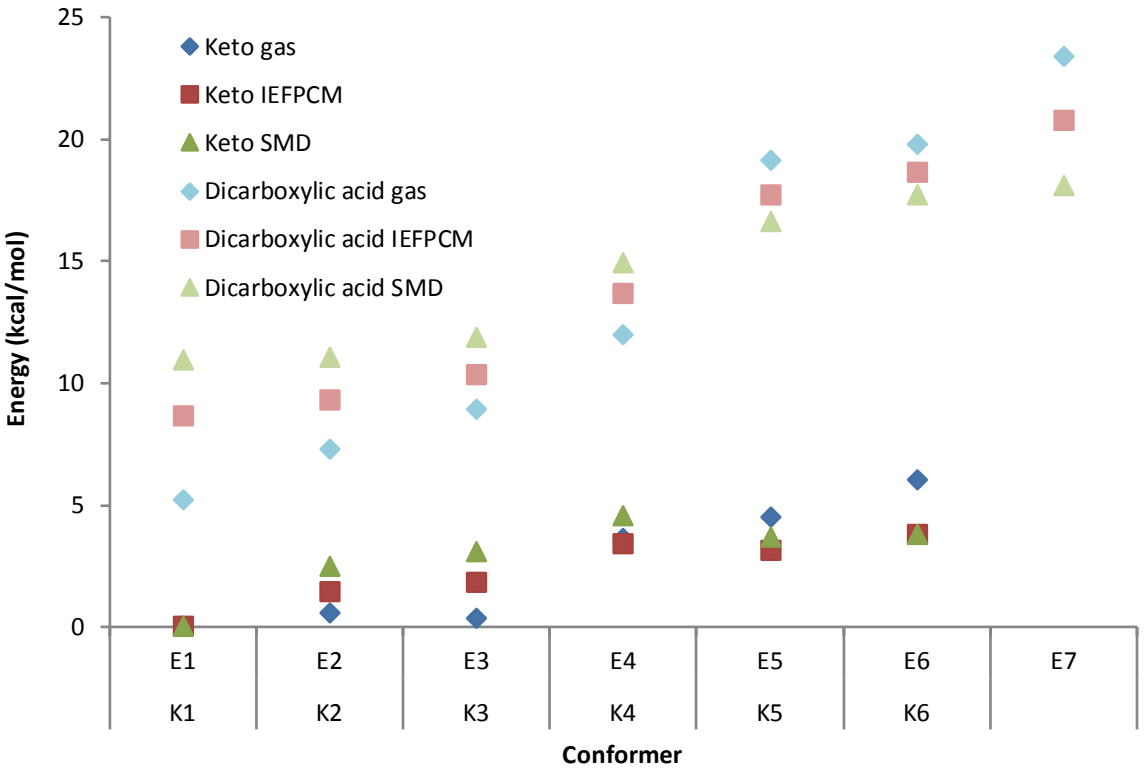

Figure 3: Gibbs energy of dicarboxylic acid and enol conformations of malonic acid, calculated at M06-2X. See Table 1 for illustrations of the conformers.

Intramolecular (direct) proton shift

The pathway for the intramolecular proton shift in malonic acid is shown in Figure 4 (with energies from other calculations in SI 021 to SI 029), and the transition state structure is illustrated in Figure 5. The model chemistries and type of energy examined vary slightly but have general agreement that there is a ~60 kcal/mol energy barrier for intramolecular (direct) proton shift. As shown in Table 2, the calculated barrier height ranges from 54.2 kcal/mol for the enthalypy at M06-2X in the gas phase, to 61.3 kcal/mol for the Gibbs energy in the M06-2X SMD aqueous model. There is a further, smaller energy barrier, as the hydrogen in enol E2 rotates around to become E1.

It is highly unlikely that malonic acid would under go an intramolecular proton shift, as the expulsion of CO_2 via a decarboxlyation mechanism has a significantly lower energy barrier; this pathway is also shown in Figure 4 and the transition state is illustrated in Figure 5. This unimolecular pathway for decarboyxlation results in energy barriers shown in Table 3; there are gas phase barriers of 27 – 30 kcal/mol and solution phase barriers of 29 – 33 kcal/mol. These results compare well to those of of Staikova et al.,[53] who calculated gas phase single molecule (non-catalysed) decarboxylation to be 26 – 28 kcal/mol, and only 20 – 22 kcal/mol if water is a catalyst.

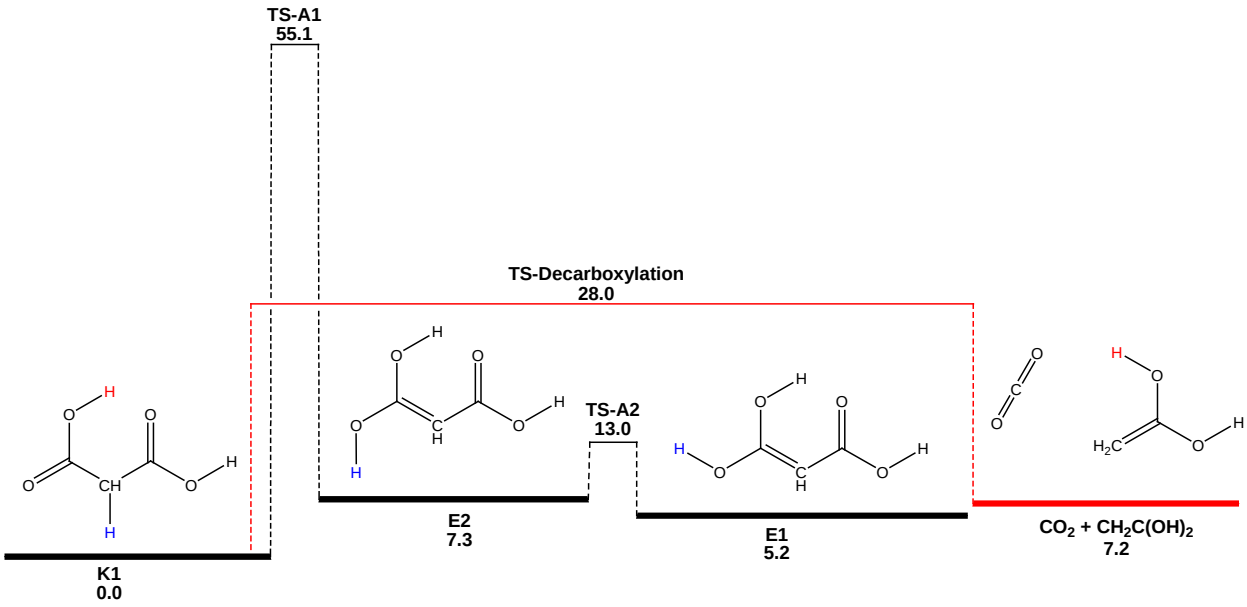

Figure 4: Energy diagram for the intramolecular keto-enol tautomerization of malonic acid (in black) and the decarboxylation of malonic acid (in red). Energies listed are Gibbs energies calculated at M05-2X/cc-pVTZ in the gas phase.

Table 2: Barrier heights (in kcal/mol) for keto-enol tautomerization of malonic acid (K1) via TS-A1.

Model Chemistry		ΔH	ΔG
	gas	54.2	55.1
M06-2X	IEF-PCM	57.7	58.8
	SMD	59.5	61.3
	gas	54.2	55.5
M05-2X	IEF-PCM	58.3	55.4
	SMD	60.2	57.0
G3SX	gas	56.2	57.2

Table 3: Relative energies (kcal/mol, compared with K1) of the energy barrier for decarboxylation.

Model Chemistry		H	G
	gas	27.2	28.0
M06-2X	IEF-PCM	29.4	29.8
	SMD	31.6	32.4
G3SX	gas	29.8	30.6

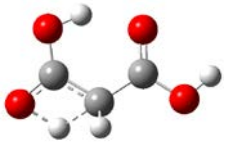

(i) Transition state for intramolecular (direct) proton exchange

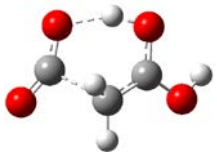

(ii) Transition state for decarboxylation

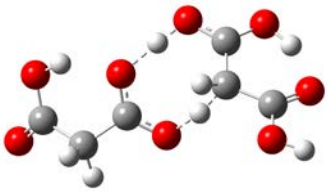

(iii) Transition state for K1

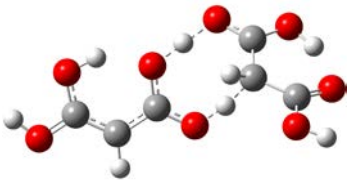

(iv) Transition state for E1

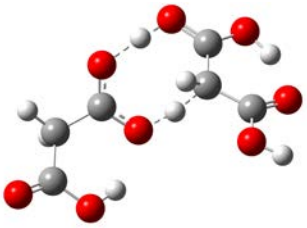

(v) Transition state for K2

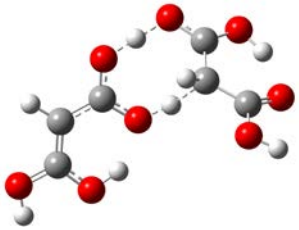

(vi) Transition state for E2

Figure 5: Illustrations of the transition state structures of (i) intramolecular (direct) proton exchange, (ii) decarboxylation and (iii) to (vi) autocatalytic keto-enol tautomerization of malonic acid.

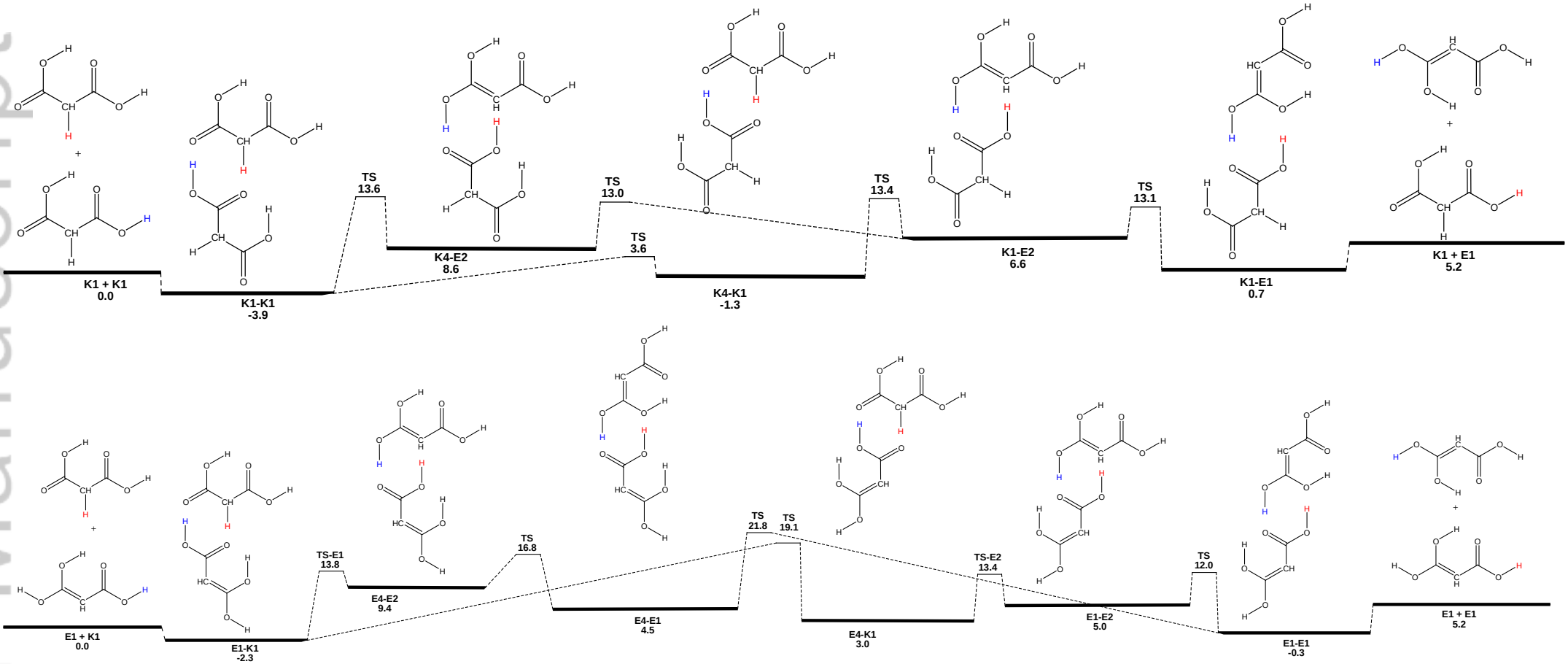

Figure 6: Acid catalysed tautomerization of malonic acid via the dicarboxylic acid (K1) and enol (E1) forms. Energies listed are Gibbs energies calculated at the M06-2X level of theory in the gas phase.

Dicarboxylic acid catalysed proton shift

Gibbs energy diagrams for keto-enol tautomerization of malonic acid catalysed by the dicarboxylic acid form of malonic acid are provided in Figure 6. The catalyst is either K1 or K4 (see Table 1), which switches from one to the other after having served as the catalyst; this process turns the reactant K1 to E2, which then relaxes to E1. The transition state structures are illustrated in Figure 5.

The four model chemistries used to compute the structures and energies in the reaction pathways follow similar trends, with some variation in relative energies. In general, M06-2X gas phase has the lowest energies, followed by G3SX, then M06-2X with the IEF-PCM solvent model and M06-2X with the SMD model. This difference is illustrated in the relative values of the energy barrier, as per Table 4 and reaction pathways in *H*, *E*+ZPE and *G* energies are shown in SI 030 to SI 046.

When looking at the enthalpies, the reaction pathways appear barrier-less (except for in SMD, in which case the main transition state is the highest energy barrier, by ~1 kcal/mol), but Gibbs energies have barrier of 13 to 26 kcal/mol, which is generally the barrier due to the double proton shift transition state, and arises due to a loss of entropy. This is tabulated in Table 4. A slightly lower energy barrier is met when K4 is used as the catalyst, compared to K1.

Table 4: Highest energy barriers in tautomerization of the dicarboxylic acid ("keto") to enol form of malonic acid when catalyzed by the keto and enol forms of malonic acid (energies reported in kcal/mol). An expanded version of this table can be found in the Supporting Information, SI 072.

Enthalpy of largest barrier								
Pathway	**M06-2X gas**		**IEF-PCM**		**SMD**		**G3SX gas**	
Keto catalyst 1: K4-K1 to K1-E2	4.1	***barrierless***	7.4	***barrierless***	9.7	K4K1 to K1E2	6.3	***barrierless***
Keto catalyst 2: K1-K1 to K4-E2	4.1	***barrierless***	7.4	***barrierless***	10.2	K1K1 to K4E2	6.3	***barrierless***
Enol catalyst 1: E4-K1 to E1-E2	9.5	E1K1 to E4K1	11.0	E1K1 to E4K1	10.4	E1K1 to E4K1	8.4	E1K1 to E4K1
Enol catalyst 2: E1-K1 to E4-E2	10.7	E4E1 to E1E1	15.5	E4E1 to E1E1	17.2	E4E1 to E1E1	12.3	E4E1 to E1E1

Gibbs Energy of largest barrier								
Pathway	**M06-2X gas**		**IEF-PCM**		**SMD**		**G3SX gas**	
Keto catalyst 1: K4-K1 to K1-E2	13.4	K4K1 to K1E2	19.5	K1E2 to K1E1	25.5	K4K1 to K1E2	18.6	K4K1 to K1E2
Keto catalyst 2: K1-K1 to K4-E2	13.6	K1K1 to K4E2	20.0	K1K1 to K4E2	26.4	K1K1 to K4E2	18.9	K1K1 to K4E2
Enol catalyst 1: E4-K1 to E1-E2	19.1	E1K1 to E4K1	20.9	E1K1 to E4K1	23.8	E4K1 to E1E2	18.6	E4K1 to E1E2

Enol catalyst 2: E1-K1 to E4-E2	21.8	E4E1 to E1E1	27.2	E4E1 to E1E1	30.1	E4E1 to E1E1	22.9	E4E1 to E1E1

Enol catalysed proton shift

Energy diagrams for keto-enol tautomerization of malonic acid catalysed by the enol form of malonic acid are provided in Figure 6 (with other calculated energies illustrated in SI 047 to SI 063). Similar to the dicarboxylic acid catalysed case, the catalyst is either E1 or E4 (see Table 1), which switches conformation across the double hydrogen shift reaction step; this process turns the reactant K1 to E2, which then relaxes to E1. These transition state structures are illustrated in Figure 5.

As listed in Table 4, the enthalpies have a barrier of ~10 kcal/mol, while in terms of Gibbs energy of the barrier heights are ~20 to 30 kcal/mol. The barrier is generally due to conformation change of the catalyst but is sometimes due to the main transition state. A slightly lower energy barrier is met when E4 is used as the catalyst, compared to E1. Both have significantly lower energy barriers than those of an intramolecular proton shift or decarboxylation but higher energy barriers than when a dicarboxylic acid form of malonic acid acts as the catalyst.

Other reaction pathways

We have seen that in the gas phase and in solution the dicarboxylic acid and enol forms of malonic acid are effective catalysts for the keto-enol tautomerization of malonic acid. It is worth noting that other reaction pathways are also possible, but have higher energy barriers. These mechanisms, for instance, involve changing the conformation of the two species once they have separated (see Figure 7 and Figure 8) or in a different order (see SI 064 to SI 071).

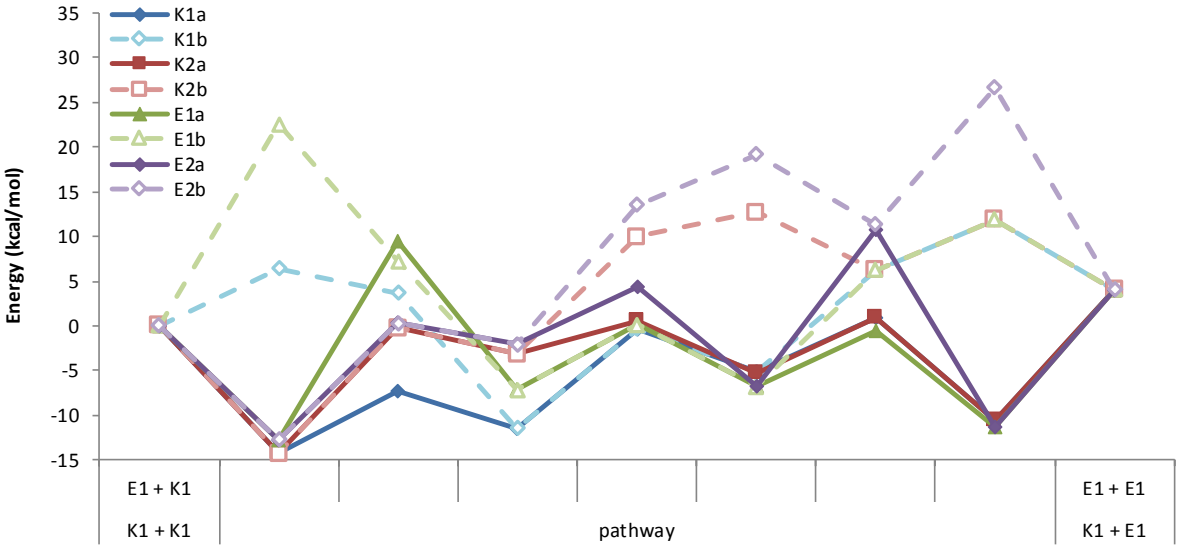

Figure 7: Enthalpy diagram for keto-enol tautomerization of malonic acid catalysed by the dicarboxylic acid (K) and enol (E) forms of malonic acid. For each catalyst, two possible reaction pathways are presented (1 and 2) as discussed above. Also illustrated is changing conformation while the catalyst and reactant are (a) interacting and (b) separate. Enthalpies are calculated at M06-2X in vacuo.

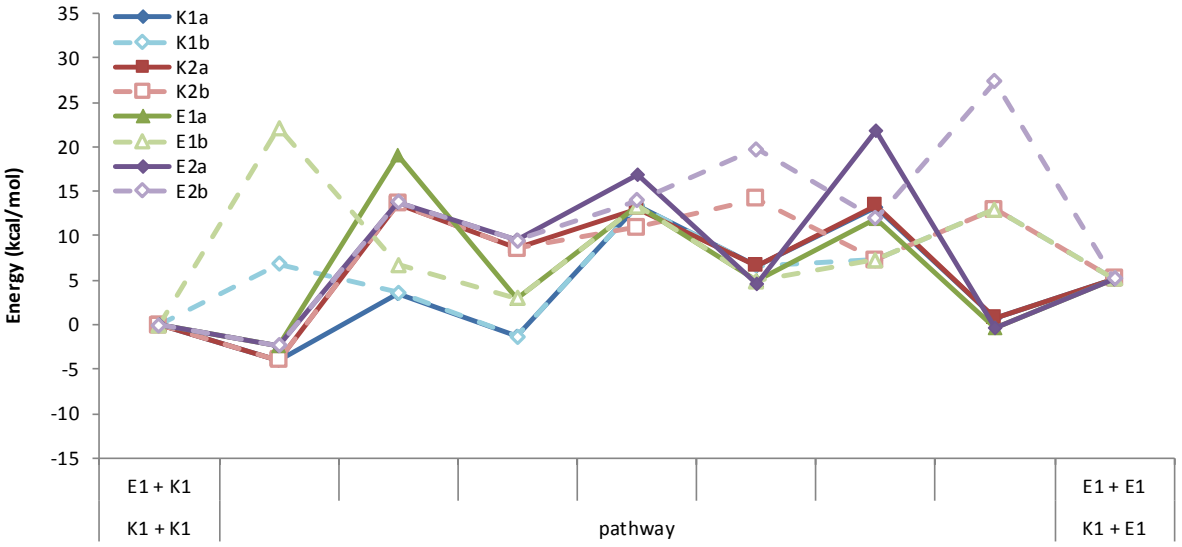

Figure 8: Energy diagram for keto-enol tautomerization of malonic acid catalysed by the dicarboxylic acid (K) and enol (E) forms of malonic acid. For each catalyst, two possible reaction pathways are presented (1 and 2) as discussed above. Also illustrated is changing conformation while the catalyst and reactant are (a) interacting and (b) separate. Energies are Gibbs energies calculated at M06-2X in vacuo.

Conclusions

This work has identified conformations of malonic acid in both dicarboxylic acid and enol forms. The most stable enol conformation (E1) is 4.1 kcal/mol higher in Enthalpy, and 5.2 kcal/mol higher in Gibbs Energy than the most stable dicarboxylic acid conformation (K1) in the gas phase. Several potential reaction pathways for the keto-enol tautomerization of malonic acid were identified. Intramolecular proton shift results in a barrier of ~60 kcal/mol, while decarboxylation has an energy barrier of ~30 kcal/mol; this suggests that in isolation, malonic acid is more likely to break apart than tautomerize to the enol form. The use of a dicarboxylic acid (K1 or K4) as a catalyst results in a reaction pathway that is barrierless in terms of enthalpy, and with Gibbs energy barrier heights of ~13 kcal in the gas phase, while there are slightly higher barriers in solution and when an enol form (E1 or E2) is used as the catalyst. Importantly, this work shows that malonic acid can undergo catalytic keto-enol tautomerization even in the absence of water, which may have implications for the composition of concentrated atmospheric aerosols.

Author Contributions

Catherine Sutton performed: writing and investigation. Chia-Yang Lim performed: conceptualization and investigation. Gabriel da Silva performed: conceptualization, investigation and writing

Funding Information

The authors are grateful to the Australian Research Council for funding through the Future Fellowship scheme (FT130101304).

References

(1) H. A. Khwaja, *Atmos. Environ.* **1995**, *29*, 127-139.
(2) L. Yang, L. E. Yu, *Environ. Sci. Technol.* **2008**, *42*, 9268-9275.
(3) S. Agarwal, S. G. Aggarwal, K. Okuzawa, K. Kawamura, *Atmos. Chem. Phys.* **2010**, *10*, 5839-5858.
(4) D. van Pinxteren, C. Neususs, H. Herrmann, *Atmos. Chem. Phys.* **2014**, *14*, 3913-3928.
(5) H. Giebl, A. Berner, G. Reischl, H. Puxbaum, A. Kasper-Giebl; R. Hitzenberger, *J. Aerosol Sci.* **2002**, *33*, 1623-1634.
(6) C. F. Braban, J. P. D. Abbatt, *Atmos. Chem. Phys.* **2004**, *4*, 1451-1459.
(7) P. G. Blower, E. Shamay, L. Kringle, S. T. Ota, G. L. Richmond, *J. Phys. Chem. A* **2013**, *117*, 2529-2542.
(8) X. Shao, Y. Zhang, S.-F. Pang, Y.-H. Zhang, *Chem. Phys.* **2017**, *483-484*, 7-11.
(9) K. R. Leopold, A. Haim, *Int. J. Chem. Kinet.* **1977**, *9*, 83.
(10) S. Ghorai, A. Laskin, A. V. Tivanski, *J. Phys. Chem. A* **2011**, *115*, 4373-4380.
(11) M. Dick-Perez, T. L. Windus, *J. Phys. Chem. A* **2017**, *121*, 2259-2264.
(12) A. R. Eberlin, D. L. H. Williams, *J. Chem. Soc.-Perkin Trans. 2* **1996**, 883-887.
(13) S. Yamabe, N. Tsuchida, K. Miyajima, *J. Phys. Chem. A* **2004**, *108*, 2750.
(14) E. Asciutto, C. Sagui, *J. Phys. Chem. A* **2005**, *109*, 7682-7687.
(15) G. da Silva, *Angew. Chem. Int. Ed.* **2010**, *49*, 7523-7525.
(16) M. Kumar, A. Sinha, J. S. Francisco, *Acc. Chem. Res.* **2016**, *49*, 877-883.
(17) M. Kumar, D. H. Busch, B. Subramaniam, W. H. Thompson, *Phys. Chem. Chem. Phys.* **2014**, *16*, 22968-22973.
(18) B. N. Du, W. C. Zhang, *Comput. Theor. Chem.* **2014**, *1049*, 90-96.
(19) A. Karton, *Chem. Phys. Lett.* **2014**, *592*, 330-333.
(20) C. R. Lin, L.-J. Yu, S. Li, Karton, A., *Chem. Phys. Lett.* **2016**, *659*, 100-104.
(21) P. P. de Castro, G. M. F. Batista, H. F. dos Santos, G. W. Amarante, *ACS Omega* **2018**, *3*, 3507-3512.
(22) A. A. Kroeger, A. Karton, *J. Comp. Chem.* **2018**, *40*, 630-637.
(23) M. Monge-Palacios, E. Grajales-Gonzalez, S. M. Sarathy, *Int. J. Quant. Chem.* **2019**, doi: 10.1002/qua.25954.
(24) M. Kumar, D. H. Busch, B. Subramaniam, W. H. Thompson, *J. Phys. Chem. A* **2014**, *118*, 5020-5028.
(25) M. Kumar, D. H. Busch, B. Subramaniam, W. H. Thompson, *J. Phys. Chem. A.* **2014**, *118*, 9701-9711.
(29) Bandyopadhyay, B., Biswas, P., *RSC Adv.* **2015**, *5*, 34588-34593.
(30) B. Bandyopadhyay, P. Biswas, P. Kumar, *Phys. Chem. Chem. Phys.* **2016**, *18*, 15995-16004.
(31) Mallick, S., Sarkar, S., Bandyopadhyay, B., Kumar, P., *Comp. Theor. Chem.* **2018**, *1132*, 50-58.
(32) S. Mallick, S. Sarkar, B. Bandyopadhyay, P. Kumar, *J. Phys. Chem. A* **2018**, *122*, 350-363.
(33) J. R. Church, R. T. Skodje, *J. Phys. Chem. A* **2018**, *122*, 5251-5260.
(34) J. M. Tadic, L. Xu, *J. Org. Chem.* **2012**, *77*, 8621-8626.
(35) B. Bandyopadhyay, P. Pandey, P. Banerjee, A. K. Samanta, T. Chakraborty, *J. Phys. Chem. A* **2012**, *116*, 3836-3845.

(36) R. J. Buszek, A. Sinha, J. S. Francisco, *J. Am. Chem. Soc.* **2011**, *133*, 2013-2015.
(37) M. K. Hazra, A. Sinha, *J. Am. Chem. Soc.* **2011**, *133*, 17444-17453.
(38) B. Long, Z. W. Long, Y. B. Wang, X. F. Tan, Y. H. Han, C. Y. Long, S. J. Qin, W. J. Zhang, *ChemPhysChem* **2012**, *13*, 323-329.
(39) Y. Wang, Y. Tang, Y. Shao, *Comp. Theor. Chem.* **2017**, *1112*, 71-81.
(40) G. Lv, X. Sun, C. Zhang, M. Li, *Atmos. Chem. Phys.* **2019**, *19*, 2833-2844.
(41) M. K. Hazra, A. Sinha, *J. Am. Chem. Soc.* **2011**, *133*, 17444-11710.
(42) B. Long, X.-F. Tan, C.-R. Chang, W.-X. Zhao, Z.-W. Long, D.-S. Ren, W.-J. Zhang, *J. Phys. Chem. A* **2013**, *117*, 5106-5116.
(43) M. K. Louie, J. S. Francisco, M. Verdicchio, S. J. Klippenstein, *J. Phys. Chem. A* **2015**, *119*, 4347-4357.
(44) S. So, U. Wille, G. da Silva, *J. Phys. Chem. A* **2015**, *119*, 9812-9820.
(45) J. Sun, S. So, G. da Silva, *Int. J. Quant. Chem.* **2017**, doi: 10.1002/qua.25434.
(46) M. J. Frisch, et al., *Gaussian 09*, Revision B.01; Gaussian Inc.: Wallingford CT, 2010.
(47) Y. Zhao, D. G. Truhlar, *Theor. Chem. Acc.* **2008**, *120*, 215-241.
(48) J. Tomasi, B. Mennucci, E. Cances, *J. Mol. Struct. THEOCHEM* **1999**, *464*, 211-226.
(49) A. V. Marenich, C. J. Cramer, D. G. Truhlar, *J. Phys. Chem. B* **2009**, *113*, 6378-6396.
(50) Y. Zhao, N. E. Schultz, D. G. Truhlar, *J. Chem. Phys.* **2005**, *123*, 161103.
(51) Y. Zhao, N. E. Schultz, D. G. Truhlar, *J. Chem. Theory Comput.* **2006**, *2*, 364-382.
(52) L. A. Curtiss, P. C. Redfern, K. Raghavachari, J. A. Pople, *J. Chem. Phys.* **2000**, *114*, 108-117.
(53) M. Staikova, M. Oh, D. J. Donaldson, *J. Phys. Chem. A* **2005**, *109*, 597-602.

Graphical Abstract

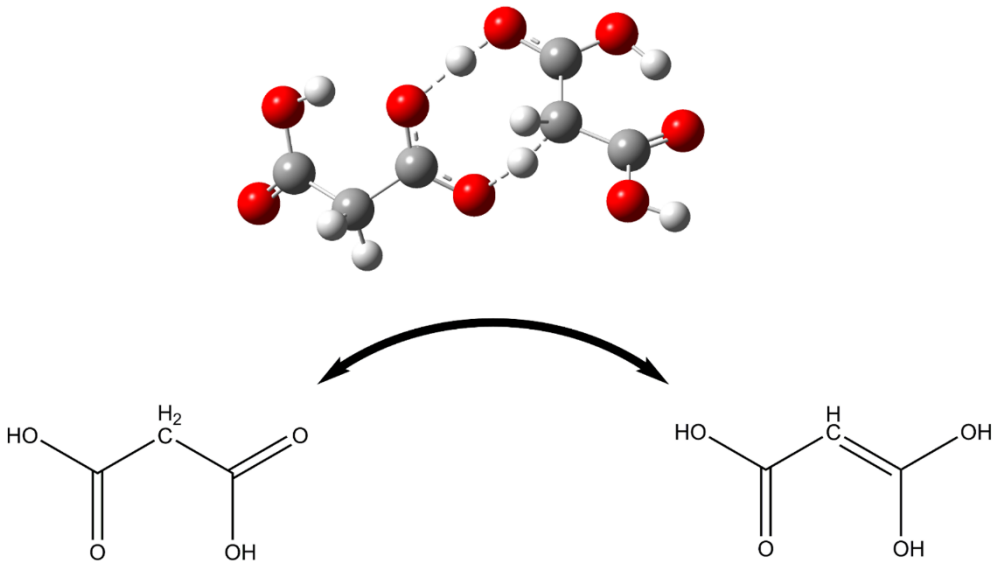

Theoretical calculations demonstrate that the tautomerisation of malonic acid is catalysed by both the acid and enol forms of malonic acid. The mechanism involves the transfer of two protons, and in aqueous media is predicted to require a barrier of 20 kcal/mol. Malonic acid is a significant component of secondary organic aerosol, where keto-enol tautomerizaztion has been observed.